Volume 51 | Number 74 | 25 September 2015 | Pages 13993–14128

ChemComm

Chemical Communications

www.rsc.org/chemcomm

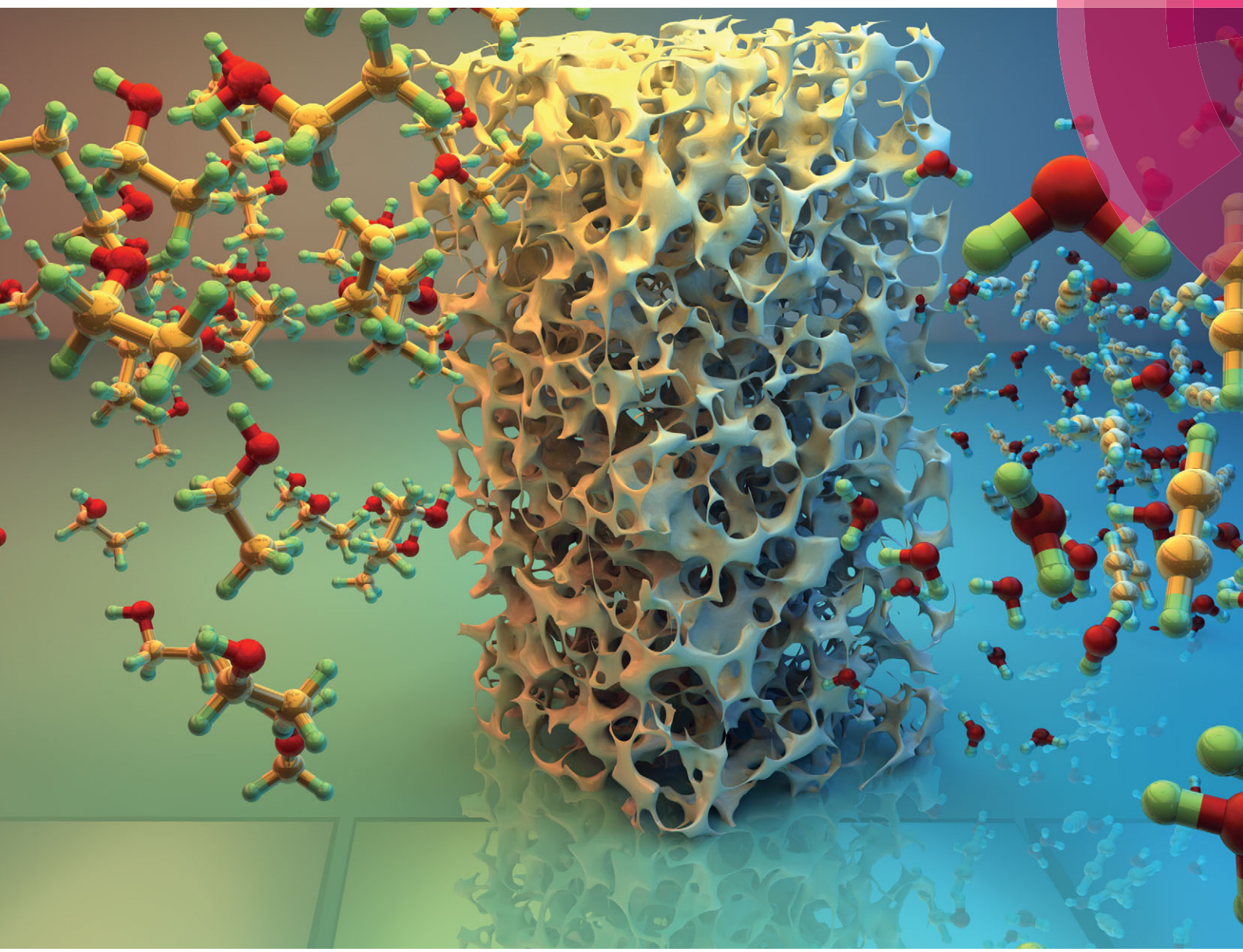

ISSN 1359-7345

ROYAL SOCIETY OF CHEMISTRY

COMMUNICATION

Damien P. Debecker, Cédric Boissière *et al.*

First acidic macro-mesocellular aluminosilicate monolithic foams "SiAl(HIPE)" and their catalytic properties

ChemComm

COMMUNICATION

View Article Online
View Journal | View Issue

Cite this: *Chem. Commun.*, 2015, **51**, 14018

Received 29th June 2015,
Accepted 29th July 2015

DOI: 10.1039/c5cc05328e

www.rsc.org/chemcomm

First acidic macro-mesocellular aluminosilicate monolithic foams "SiAl(HIPE)" and their catalytic properties†

Damien P. Debecker,*[a] Cédric Boissière,*[b] Guillaume Laurent,[b] Stéphanie Huet,[c] Philippe Eliaers,[d] Clément Sanchez[b] and Rénal Backov[c]

A new type of acidic macrocellular and mesoporous silica–alumina foam is obtained *via* a one pot alkaline sol–gel route coupled with a concentrated emulsion-based templating technique. The mixed oxide monolith exhibits high surface acidity, translating into excellent performance in the acid-catalyzed dehydration of bioethanol to ethene.

Aluminosilicates are of utmost importance as catalysts and catalyst supports.[1] Amorphous aluminosilicates are used as mild acidic supports for various active species such as, for instance, Mo, W or Re oxides for olefin metathesis;[2] Ni, W, Co and Mo oxides for hydrodesulfurization reactions;[3] Ni for reduction reactions;[4] Pd and Pt for hydrogenation reactions,[5] *etc.* They are also employed as catalysts themselves in several petrochemical processes, including cracking.[6] Their acidity can be somewhat tuned to meet the specific requirement of a particular reaction.

Zeolites are synthetic microporous crystalline aluminosilicates, in which Al atoms replace Si atoms in the framework, thereby generating uncompensated charge and strong acidity.[1a] Even if their composition, acidity and structure can be finely tuned, zeolites usually exhibit only small pores in which the diffusion of reactants and products is hampered. Significant steps forward have been made in the design of truly mesoporous acidic aluminosilicates when templating agents have been used to generate mesopores in zeolitic materials.[7] Further developments in this field are still flourishing, taking benefits of advanced polymer science or original processing techniques.[8]

Nevertheless, whether amorphous or crystalline, micro- or mesoporous, catalytic materials in the form of powders have to be shaped as extrudates, pellets or monoliths before being used in industrial flow processes.[9] This step is usually not straightforward, as (i) appropriate additives must be found that ensure physical strength without compromising catalytic performance, (ii) diffusion limitation issues must be addressed and (iii) attrition must be avoided.[10] An alternative to shaping powders is to impregnate structured supports with active components.[11] There also, potential technical issues are numerous: lack of adherence of the catalytic powder to the walls of the structured support, pore plugging, drastic decrease of the specific loading and so forth.

One-step preparation of structured materials with the required properties is hence highly desirable. In this context, the integration of sol–gel chemistry and physical chemistry of complex fluids has led to the genesis of various advanced functional materials.[12] The one-step preparation of macrocellular silica monoliths is a noteworthy example.[13] Taking advantage of sol–gel chemistry coupled with an emulsion technique, macroscopic silica blocks of defined shape can be obtained, featuring high surface area and good mechanical strength (5–7 MPa Young's modulus).[14] The preparation is based on the 'High Internal Phase Emulsion' (HIPE) method.[15] Si(HIPE) can be prepared as self-standing macroscopic objects that can be easily manipulated. Along with other diverse applications, these materials when hybridized[15] proved to be successful as catalyst supports for lipases used in oleochemistry,[16] for Pd nanoparticles used in C–C coupling,[17] *etc.* Such materials can be cast directly in tubular reactors and be employed as catalyst supports for flow reactions even with bulky molecules.[18]

The incorporation of alumina into such a system would pave the way to structured acid catalysts. However, this is not straightforward since chemical synthesis conditions used for the preparation of such materials are systematically based on colloidal or acidic silica chemistry. The latter routes are totally inefficient for the true incorporation of aluminum cationic species into the silica network.[19] While Al in tetrahedral

[a] *Institute of Condensed Matter and Nanoscience - Molecules, Solids and reactiviTy (IMCN/MOST), Université catholique de Louvain, Croix du Sud 2/17, 1348 Louvain-La-Neuve, Belgium. E-mail: damien.debecker@uclouvain.be*
[b] *Sorbonne Universités, UPMC Univ Paris 06, CNRS, Collège de France, Laboratoire de Chimie de la Matière Condensée de Paris (LCMCP), 11 place Marcelin Berthelot, 75005, Paris, France. E-mail: cedric.boissiere@upmc.fr*
[c] *Centre de Recherche Paul Pascal, UPR8641, Université de Bordeaux 1, 115 Avenue Albert Schweitzer, 33600 Pessac, France*
[d] *Certech (Centre de Ressources Technologiques en Chimie), rue Jules Bordet, 7180 Seneffe, Belgium*

† Electronic supplementary information (ESI) available: Full experimental details and additional data. See DOI: 10.1039/c5cc05328e

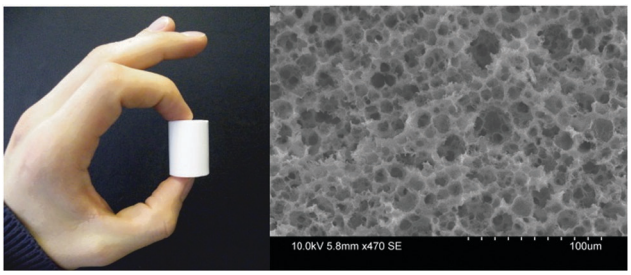

Fig. 1 (left) Picture of a SiAl(HIPE) monolith, (right) SEM micrograph of the SiAl(HIPE).

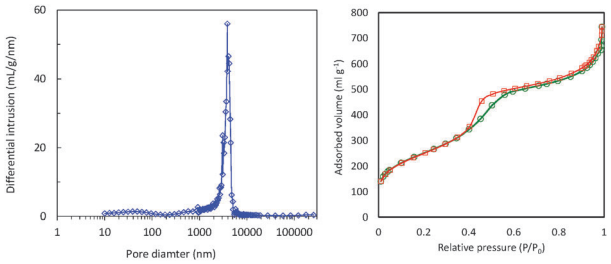

Fig. 2 (left) Size distribution of the macroscopic pore opening obtained by mercury intrusion porosimetry and (right) N_2-sorption isotherms.

coordination is required to obtain strongly acid heterogeneous catalysts,[20] classical routes usually generate aluminum oxide chunks in an octahedral environment.

In the present study the emulsion-based sol–gel route is modified in an alkaline version to meet the ambitious agenda of obtaining, in one-step, a structured monolithic acidic catalyst bearing hierarchical porosity. The adapted protocol is described in detail in the ESI.† Briefly, TEOS is incorporated into the emulsion oil phase (dodecane) along with the TTAB surfactant. Aluminum isopropoxide is added in the water phase along with TPAOH. A stable emulsion is formed after vigorous stirring and is simply allowed to stand for 1 week, washed and calcined. In this way, SiAl(HIPE) was prepared in the form of cm-scale solid monoliths (Fig. 1 and ESI†). Macroscopically, SiAl(HIPE) materials appear similar to Si(HIPE).

Pieces of monolith were scratched and observed using scanning electron microscopy (SEM). This revealed the macrocellular structure of the materials (Fig. 1). Interconnected macro-cells have a diameter in the 5–45 μm range. As compared to the well-described Si(HIPE) materials, these macrocells are smaller and present a narrower pore size distribution. This can tentatively be associated with the fact that the SiAl(HIPE) monoliths have been obtained in alkaline pH. Under these conditions, condensation reactions are expected to proceed at a faster rate, generating high shearing forces earlier in the emulsion process, thus minimizing the oil droplet diameters and favoring size monodispersity.[14] The atomic Si/Al ratio was estimated over several wide zones of different monolith pieces using the EDX probe mounted on the SEM apparatus to be 9.7 ± 0.2, not very far from the nominal value of 12. Possibly, a portion of the TEOS did not react at the oil/water interface and was eliminated during the washing. The composition was shown to be fairly homogeneous throughout the sample (ESI†). The sample is macroporous as attested using SEM and confirmed by Hg-porosimetry (Fig. 2). SiAl(HIPE) is characterized by an intrusion volume of 10.2 $cm^3\ g^{-1}$ and a porosity of 89%. Its bulk density is 0.087 g cm^{-3}. In terms of macrostructures, the alkaline synthesis method allows the production of materials that are as good as those previously reported Si(HIPE). However, the skeletal density obtained is only 0.80 g cm^{-3}, which is lower than Si(HIPE) (~1.50 g cm^{-3}). Macrocells are interconnected by relatively monodisperse pore openings around 4 μm in size.

N_2-physisorption measurements demonstrate that SiAl(HIPE) is mesoporous. The BET surface area reaches 900 $m^2\ g^{-1}$. Contrary to the Si(HIPE) series, a *t*-plot analysis of the isotherm proves that no significant microporosity is present in this material, the nitrogen uptake at very low relative pressure being attributed to the high surface area of the samples. A well-defined hysteresis loop in the isotherms translates into a sharp pore size distribution obtained from the adsorption branch, centered at *ca.* 3.6 nm *via* the BJH method, and 4.0 nm *via* the Broekhoff and De Boer method (ESI†). The presence of a so-called catastrophic desorption at $P/P_0 \sim 0.42$ make the estimation of the mesopores restriction size impossible.

The sample acidity was measured using NH_3-chemisorption and compared to both a popular commercial aluminosilicate support (Aldrich, Grade 135, 475 $m^2\ g^{-1}$, 12 wt% Al_2O_3)[22] and Si(HIPE)[17b] (Fig. 3). The method allows a quantitative analysis of acid sites, with a distinction between the weak and the strong sites.[21] As expected, Si(HIPE) is virtually not acidic. Aluminosilicate samples on the other hand retain NH_3 in substantial quantities and SiAl(HIPE) exhibited a total number of acid sites per gram of a sample significantly higher than the reference commercial aluminosilicate. The amount of strong acidic sites is almost 3-fold as compared to that of the reference. If the two aluminosilicate materials are compared on a surface basis, the reference exhibits more acidic sites. However, SiAl(HIPE) still exhibits more strong acid sites per surface unit.

NMR experiments were conducted to gain insights into the environment of Si and Al atoms in SiAl(HIPE). It appears important, indeed, to verify that the sol–gel process performed in basic pH did not lead to the stabilization of alumina domains dispersed in a silica matrix, but that a truly mixed oxide was formed instead. ^{29}Si MAS NMR spectra (Fig. 4) show broader peaks strongly shifted to the left, which is typical for aluminosilicates.[23] This shows that Si and Al precursors have reacted together during the preparation to form Si–O–Al bonds.

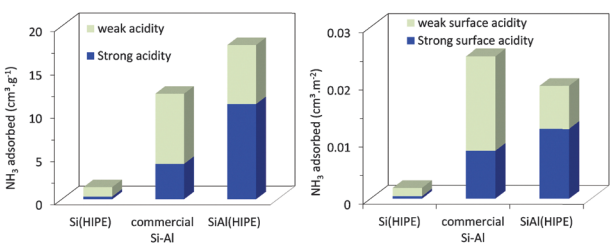

Fig. 3 Acidity of SiAl(HIPE) measured using NH_3-chemisorption[21] and compared to the commercial reference and to Si(HIPE). The acidity is expressed as the amount of NH_3 chemisorbed per gram of catalyst (left) or per m^2 of catalyst (right).

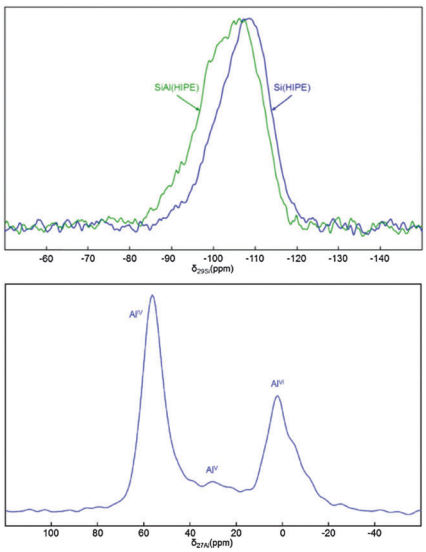

Fig. 4 (up) ^{29}Si MAS-NMR spectra of Si(HIPE) and SiAl(HIPE) and (bottom) ^{27}Al MAS-NMR spectrum of SiAl(HIPE).

The ^{27}Al MAS-NMR spectrum obtained for SiAl(HIPE) shows a large proportion of tetrahedrally coordinated framework Al atoms (signal at *ca.* 56 ppm, abbreviated Al^{IV}). The latter is typically formed in amorphous aluminosilicates, along with pentacoordinated Al (broad signal around 30 ppm, abbreviated Al^{V}) and octahedral Al (*ca.* 2 ppm, abbreviated Al^{VI}).[2a,24] In SiAl(HIPE), however, the proportion of Al^{IV} species *versus* Al^{V} and Al^{VI} is significantly higher than what is typically found in the reference aluminosilicate.[25]

Such a high content of Al^{IV} species is characteristic of pre-zeolitic amorphous aluminosilicate materials prepared in basic media under similar conditions.[19] As a consequence, one may explain both the sol–gel condensation and the good incorporation of aluminum centers within the silica network by the progressive dodecane/water interfacial hydrolysis of TEOS and deprotonation of silicic acid that locally induces a pH drop (Fig. 5), allowing the polycondensation of fleeting aluminum hydroxide with silicate species. Both TEOS and TTAB diffusion within the dodecane phase and aluminate diffusion within the aqueous phase being slow, there is time for a progressive self-assembly of the positively charged TTAB structuring agent and negatively charged alumino-silicate oligomers, resulting in the mesostructured SiAl(HIPE).

An interesting feature of solid state NMR spectroscopy is the possibility of checking spatial proximities between nuclei. For quadrupolar nuclei like ^{27}Al, the TRAPDOR experiment can be used.[27] This has been undertaken on a dehydrated sample to discriminate which protons are neighboring ^{27}Al centers and thus which ones are expected to be implicated in the catalytic activity. The experiment consists of comparing two spectra, a reference one without ^{27}Al irradiation and an irradiated one, at increasing echo times. The closer the involved spins, the higher will be the dephasing effect. A strong effect is observed around 5 ppm, corresponding to Si–(OH)–Al hydrogen-bonded species; an intermediate effect is seen at 2–2.5 ppm, attributed to Si–OH close to the Al center; and no effect is denoted for isolated Si–OH at 1.8 ppm (Fig. 6). Thus, the strong Si–O–Al Brönsted acidity observed here matches the high standard of some already reported powdery materials produced by precipitation or aerosol processing, like those obtained from zeolite seeds or amorphous prezeolitic materials.[19]

From catalytic point of view, both the SiAl(HIPE) and the reference materials catalyze the dehydration of ethanol with high selectivity (~95%) under the conditions used here (Fig. 7). For SiAl(HIPE), conversion remains almost complete up to a space velocity (WHSV) of 23.8 h^{-1}. Note that longer contact times are classically reported in the literature.[28] Under our conditions and with a WHSV of 23.8 h^{-1}, the specific productivity reaches 13.3 $g_{ethene}\ g_{cat}^{-1}\ h^{-1}$ for SiAl(HIPE), while the commercial sample produces only 10.4 $g_{ethene}\ g_{cat}^{-1}\ h^{-1}$. As the dehydration of ethanol is known to occur on acid sites, such high ethene productivity is related to the enhanced acidic properties of the SiAl(HIPE). By-products include butenes, acetaldehyde and diethyl ether. The full product selectivity profile is provided in the ESI.† Acetaldehyde selectivity systematically remained below 0.5%. While diethyl ether is obtained *via* a less complete dehydration of ethanol, 1-butene is the product of a consecutive dimerization reaction of ethylene. Thus, as expected, selectivity for diethyl ether was lower and 1-butene selectivity was higher for SiAl(HIPE) as

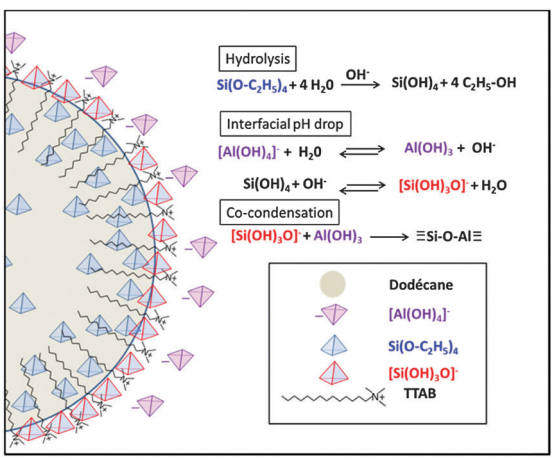

Fig. 5 Diffusion-limited sol–gel aluminosilicate co-condensation mechanism taking place at the dodecane/water interface.

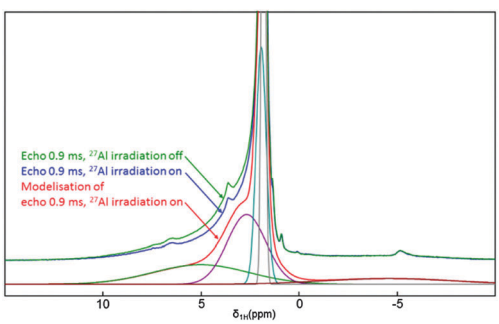

Fig. 6 Echo MAS ^{1}H NMR spectra (sample dehydrated at 200 °C). The chemical shift is based on the {^{27}Al}-^{1}H TRAPDOR experiment (spectra were simulated using dmfit program;[26] see the ESI†)

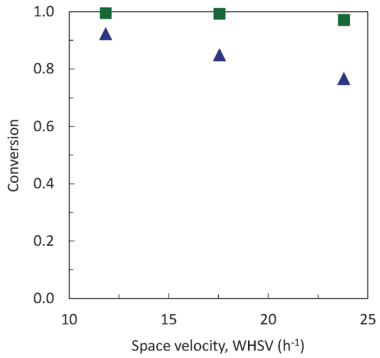

Fig. 7 Conversion of ethanol at 400 °C with (■) SiAl(HIPE) and (▲) the reference. 1.2 g of the catalyst. Selectivity to ethanol is always in the range of 94.2–97.6% (see Table S1, ESI,† for a full product profile). Feed is first generation bioethanol from BioWanze; 99.7 wt% ethanol and −0.3 wt% water evaporated in a preheating zone.

compared to the commercial reference. This again points to a higher acidity and thus a higher activity of the SiAl(HIPE).

Combining sol–gel chemistry and physical chemistry of complex fluids, the new route presented here allows the preparation of meso-macrocellular self-standing objects that are easy to cast and manipulate and that exhibit open and interconnected macro-porosity, high surface area and strong acidic properties. The textural and structural features of these new aluminosilicate monoliths make them particularly attractive for flow processes. The formation of a true mixed aluminosilicate generates abundant and strong surface acid sites, which makes these materials highly attractive for acid-catalyzed reactions. Effectiveness of these catalysts is demonstrated here in the case of bioethanol dehydration, and good performance can be expected in other processes involving bulkier molecules like cracking, isomerization, and alkylation reactions.

The French Région Ile de France SESAME program is acknowledged for financial support (700 MHz spectrometer).

Notes and references

1 (*a*) A. Corma, *Chem. Rev.*, 1995, **95**, 559; (*b*) G. Busca, *Chem. Rev.*, 2007, **107**, 5366.
2 (*a*) D. P. Debecker, M. Stoyanova, U. Rodemerck, P. Eloy, A. Léonard, B.-L. Su and E. M. Gaigneaux, *J. Phys. Chem. C*, 2010, **114**, 18664; (*b*) B. B. Marvey, *Int. J. Mol. Sci.*, 2009, **10**, 213; (*c*) K. Bouchmella, P. Hubert Mutin, M. Stoyanova, C. Poleunis, P. Eloy, U. Rodemerck, E. M. Gaigneaux and D. P. Debecker, *J. Catal.*, 2013, **301**, 233.
3 (*a*) E. J. M. Hensen, D. G. Poduval and J. A. R. van Veen, *Ind. Eng. Chem. Res.*, 2007, **46**, 4202; (*b*) T. I. Koranyi and J. B. Nagy, *React. Kinet. Catal. Lett.*, 2005, **85**, 131.
4 I. H. A. El Maksod, E. Z. Hegazy, S. H. Kenawy and T. S. Saleh, *Adv. Synth. Catal.*, 2010, **352**, 1169.
5 (*a*) K. Ezuka, M. Ohshima, H. Kurokawa and H. Miura, *J. Jpn. Pet. Inst.*, 2009, **52**, 10; (*b*) E. Peeters, M. Cattenot, C. Geantet, M. Breysse and J. L. Zotin, *Catal. Today*, 2008, **133**, 299.
6 (*a*) A. Ishihara, H. Negura, T. Hashimoto and H. Nasu, *Appl. Catal., A*, 2010, **388**, 68; (*b*) M. A. Ali, T. Tatsumi and T. Masuda, *Appl. Catal., A*, 2002, **233**, 77; (*c*) R. Mokaya and W. Jones, *J. Catal.*, 1997, **172**, 211; (*d*) R. Takahashi, S. Sato, T. Sodesawa and M. Yabuki, *J. Catal.*, 2001, **200**, 197.
7 C. T. Kresge, M. E. Leonowicz, W. J. Roth, J. C. Vartuli and J. S. Beck, *Nature*, 1992, **359**, 710.
8 (*a*) D. P. Debecker, M. Stoyanova, F. Colbeau-Justin, U. Rodemerck, C. Boissière, E. M. Gaigneaux and C. Sanchez, *Angew. Chem., Int. Ed.*, 2012, **51**, 2129; (*b*) X. Zhou, S. Song, A. Duan, Z. Zhao, Y. Gong, X. Wang, J. Li, Y. Wei, G. Jiang and J. Liu, *ChemCatChem*, 2015, **7**, 1948–1960; (*c*) F. Colbeau-Justin, C. Boissière, A. Chaumonnot, A. Bonduelle and C. Sanchez, *Adv. Funct. Mater.*, 2014, **24**, 233; (*d*) M. Fujiwara, A. Sakamoto, K. Shiokawa, A. K. Patra and A. Bhaumik, *Microporous Mesoporous Mater.*, 2011, **142**, 381; (*e*) X. Meng, F. Nawaz and F.-S. Xiao, *Nano Today*, 2009, **4**, 292; (*f*) C. Boissiere, D. Grosso, A. Chaumonnot, L. Nicole and C. Sanchez, *Adv. Mater.*, 2011, **23**, 599; (*g*) X. Xu, T. Zhao, J. Qi, Y. Guo, C. Miao, F. Li and M. Liang, *Mater. Lett.*, 2010, **64**, 1660; (*h*) M. Falco, J. Retuert, A. Hidrobo, C. Covarrubias, P. Araya and U. Sedran, *Appl. Catal., A*, 2009, **366**, 269.
9 S. Mitchell, N.-L. Michels, K. Kunze and J. Pérez-Ramírez, *Nat. Chem.*, 2012, **4**, 825.
10 (*a*) V. G. Baldovino-Medrano, M. T. Le, I. Van Driessche, E. Bruneel, C. Alcázar, M. T. Colomer, R. Moreno, A. Florencie, B. Farin and E. M. Gaigneaux, *Catal. Today*, 2015, **246**, 81; (*b*) C. Ngamcharussrivichai, W. Meechan, A. Ketcong, K. Kangwansaichon and S. Butnark, *J. Ind. Eng. Chem.*, 2011, **17**, 587.
11 (*a*) T. A. Nijhuis, A. E. W. Beers, T. Vergunst, I. Hoek, F. Kapteijn and J. A. Moulijn, *Catal. Rev.: Sci. Eng.*, 2001, **43**, 345; (*b*) F. E. Tuler, E. D. Banús, M. A. Zanuttini, E. E. Miró and V. G. Milt, *Chem. Eng. J.*, 2014, **246**, 287; (*c*) A. Sachse, V. Hulea, A. Finiels, B. Coq, F. Fajula and A. Galarneau, *J. Catal.*, 2012, **287**, 62.
12 (*a*) R. Backov, *Soft Matter*, 2006, **2**, 452; (*b*) C. Sanchez, P. Belleville, M. Popall and L. Nicole, *Chem. Soc. Rev.*, 2011, **40**, 696.
13 A. El Kadib, R. Chimenton, A. Sachse, F. Fajula, A. Galarneau and B. Coq, *Angew. Chem., Int. Ed.*, 2009, **48**, 4969.
14 F. Carn, A. Colin, M.-F. Achard, H. Deleuze, E. Sellier, M. Birot and R. Backov, *J. Mater. Chem.*, 2004, **14**, 1370.
15 N. Brun, S. Ungureanu, H. Deleuze and R. Backov, *Chem. Soc. Rev.*, 2011, **40**, 771.
16 N. Brun, A. B. Garcia, H. Deleuze, M. F. Achard, C. Sanchez, F. Durand, V. Oestreicher and R. Backov, *Chem. Mater.*, 2010, **22**, 4555.
17 (*a*) S. Ungureanu, H. Deleuze, O. Babot, M. F. Achard, C. Sanchez, M. I. Popa and R. Backov, *Appl. Catal., A*, 2010, **390**, 51; (*b*) S. Ungureanu, H. Deleuze, C. Sanchez, M. I. Popa and R. Backov, *Chem. Mater.*, 2008, **20**, 6494.
18 N. Brun, A. Babeau-Garcia, M. F. Achard, C. Sanchez, F. Durand, G. Laurent, M. Birot, H. Deleuze and R. Backov, *Energy Environ. Sci.*, 2011, **4**, 2840.
19 S. Pega, C. Boissière, D. Grosso, T. Azaïs, A. Chaumonnot and C. Sanchez, *Angew. Chem., Int. Ed.*, 2009, **48**, 2784.
20 G. Busca, *Metal Oxides as Acid-Base Catalytic Materials*, Elsevier, Amsterdam, 2014, ch. 6.
21 D. P. Debecker, D. Hauwaert, M. Stoyanova, A. Barkschat, U. Rodemerck and E. M. Gaigneaux, *Appl. Catal., A*, 2011, **391**, 78.
22 D. P. Debecker, M. Stoyanova, U. Rodemerck, A. Leonard, B.-L. Su and E. M. Gaigneaux, *Catal. Today*, 2011, **169**, 60.
23 G. J. Kennedy, J. W. Wiench and M. Pruski, *Solid State Nucl. Magn. Reson.*, 2008, **33**, 76.
24 E. J. M. Hensen, D. G. Poduval, P. C. M. M. Magusin, A. E. Coumans and J. A. R. van Veen, *J. Catal.*, 2010, **269**, 201.
25 (*a*) D. P. Debecker, M. Stoyanova, U. Rodemerck and E. M. Gaigneaux, *J. Mol. Catal. A: Chem.*, 2011, **340**, 65; (*b*) M. May, M. Asomoza, T. Lopez and R. Gomez, *Chem. Mater.*, 1997, **9**, 2395.
26 D. Massiot, F. Fayon, M. Capron, I. King, S. Le Calvé, B. Alonso, J.-O. Durand, B. Bujoli, Z. Gan and G. Hoatson, *Magn. Reson. Chem.*, 2002, **40**, 70.
27 C. P. Grey and A. J. Vega, *J. Am. Chem. Soc.*, 1995, **117**, 8232.
28 (*a*) J. Bi, X. Guo, M. Liu and X. Wang, *Catal. Today*, 2010, **149**, 143; (*b*) D. Fan, D.-J. Dai and H.-S. Wu, *Materials*, 2012, **6**, 101; (*c*) M. Zhang and Y. Yu, *Ind. Eng. Chem. Res.*, 2013, **52**, 9505.